Resistively detected high-order magnetoplasmons in a high-quality two-dimensional electron gas

Q. Shi,[1] M. A. Zudov,[1,*] L. N. Pfeiffer,[2] K. W. West,[2] J. D. Watson,[3,4] and M. J. Manfra[3,4,5,6]

[1]*School of Physics and Astronomy, University of Minnesota, Minneapolis, Minnesota 55455, USA*

[2]*Princeton University, Department of Electrical Engineering, Princeton, New Jersey 08544, USA*

[3]*Department of Physics and Astronomy, Purdue University, West Lafayette, Indiana 47907, USA*

[4]*Birck Nanotechnology Center, Purdue University, West Lafayette, Indiana 47907, USA*

[5]*School of Materials Engineering, Purdue University, West Lafayette, Indiana 47907, USA*

[6]*School of Electrical and Computer Engineering, Purdue University, West Lafayette, Indiana 47907, USA*

We report on high-order magnetoplasmon resonances detected in photoresistance in high-mobility GaAs quantum wells. These resonances manifest themselves as a series of photoresistance extrema in the regime of Shubnikov–de Haas oscillations. Extending to orders as high as 25, the extrema exhibit alternating strength, being less (more) pronounced at even- (odd-)order magnetoplasmon modes. This experimental technique provides a sensitive and elegant means to detect and investigate multiple magnetoplasmon modes and could be applied to other systems.

When a two-dimensional electron gas (2DEG), laterally confined to a Hall bar of width w, is subjected to a weak perpendicular magnetic field B and microwave radiation, its photoresistance reveals magnetoplasmon resonances (MPRs) [1–11]. The nth plasmon mode has a wave number $q_n = \pi n/w$ ($n = 1,2,\ldots$) and, due to the hybridization with the cyclotron mode in a magnetic field, its dispersion takes the form [12,13]

$$\omega_n = \sqrt{\omega_c^2 + \Omega_n^2}, \quad \Omega_n^2 = n\Omega_1^2, \quad \Omega_1^2 = \frac{2\pi\alpha c}{\epsilon^\star w}\frac{E_F}{\hbar}. \quad (1)$$

Here, $\omega_c = eB/m^\star$ is the cyclotron frequency of an electron with the effective mass $m^\star$, $\Omega_1 = 2\pi F_1$ is the frequency of the plasmon mode with the wave number π/w, $\alpha = e^2/4\pi\epsilon_0\hbar c \approx 1/137$ is the fine-structure constant, ϵ_0 is the vacuum permittivity, $\epsilon^\star = (\epsilon + 1)/2$ is the effective dielectric constant of the surrounding medium, $\epsilon = 12.8$ is the dielectric constant of GaAs, and E_F is the Fermi energy. The MPRs occur when the excitation frequency $\omega = 2\pi f$ is equal to ω_n, which can be tuned by B.

Although there exists no quantitative theory of the MPR photoresistance, it is believed that the radiation absorption translates to electron heating which, in turn, causes a resistivity change [1,4,6]. While some photoresistance measurements revealed either only the fundamental [1] or the lowest few odd-order MPR modes [4], another study [6] reported MPR modes with $n = 1,2,3,4$. Higher-order ($n \lesssim 10$) MPRs have been observed in microwave absorption [14] and spatially resolved photoluminescence [15] and, more recently, even higher modes have been detected in photovoltage [16,17] and differential luminescence spectra [18].

Since the number of observable MPR modes is given by $(f/F_1)^2$, high excitation frequency f is a prerequisite for the observation of high-order modes. In addition, for the MPR modes to be experimentally resolved, the spacing between them should exceed their width. The half width of the nth

MPR can be written as [19–21]

$$\delta\omega_n = \gamma + \Gamma_n, \quad (2)$$

where γ is the incoherent scattering rate and Γ_n is the super-radiant rate due to coherent dipole reradiation of oscillating two-dimensional (2D) electrons. The super-radiant decay rate Γ_n is given by [22]

$$\Gamma_n = \Gamma_0(L_n/\lambda)^2, \quad \Gamma_0 = \frac{2\alpha}{n^\star}\frac{E_F}{\hbar}, \quad (3)$$

where L_n is the coherence length, $\lambda = c/fn^\star$ is the photon wavelength, and $n^\star = (\sqrt{\epsilon} + 1)/2$ is the effective refractive index. At high n, the super-radiant rate drops rapidly due to the decay of coherence length $L_n \sim w/n$ [18] and the MPR width is governed by the incoherent rate γ. Therefore, a small incoherent scattering rate is another essential ingredient for the detection of high-order MPRs.

Here we report on very high-order magnetoplasmon resonances resistively detected in very high-quality GaAs quantum wells at radiation frequencies up to ~ 0.4 THz. Owing to the high sensitivity of Shubnikov–de Haas oscillations (SdHOs) to MPR-induced changes of electron temperature, the resonances manifest themselves as a series of resistance extrema superimposed on the SdHOs. Extending to orders as high as $n = 25$, the extrema exhibit alternating strength, being less (more) pronounced at even (odd) magnetoplasmon modes. The employed experimental scheme provides a very efficient way to investigate the properties of MPRs and could be applicable to other 2D systems.

Our samples are 200-μm-wide Hall bars fabricated from symmetrically doped, 30-nm-wide GaAs/AlGaAs quantum wells. After low-temperature illumination, the electron density and mobility of a Princeton-grown sample A were $n_e \approx 2.5 \times 10^{11}$ cm^{-2} and $\mu \approx 2.5 \times 10^7$ cm^2/Vs, respectively. Sample B, grown at Purdue, had $n_e \approx 2.6 \times 10^{11}$ cm^{-2} and $\mu \approx 1.3 \times 10^7$ cm^2/Vs. The resistivity was measured at temperatures of 0.3–0.4 K using a standard low-frequency lock-in technique, in sweeping B and under radiation of frequency f from 0.23 to 0.38 THz generated by a backward wave oscillator.
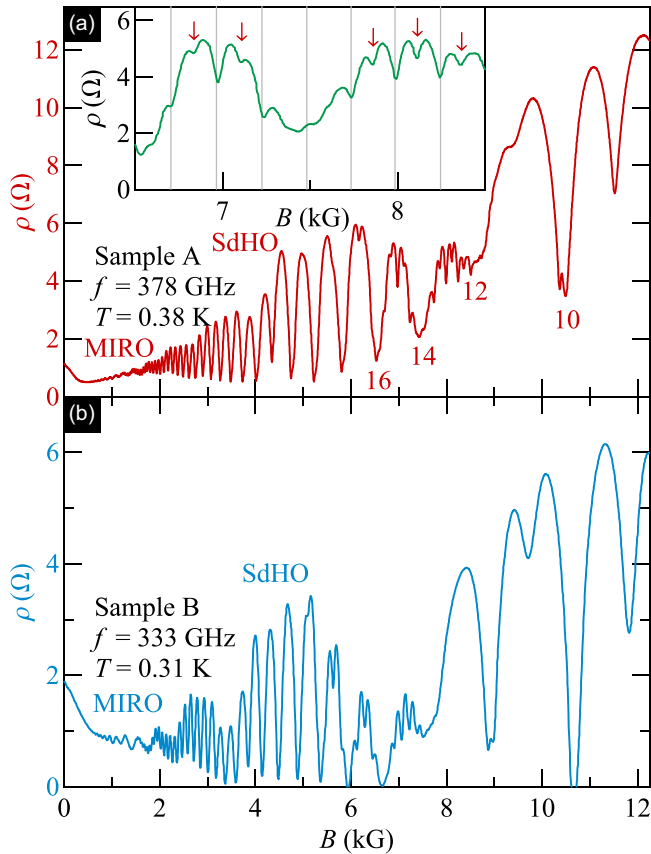
*Corresponding author: zudov@physics.umn.edu

FIG. 1. (a) [(b)] $\rho(B)$ measured in sample A [B] at $f = 378$ [333] GHz and $T \approx 0.38$ [0.31] K. SdHO minima in (a) are marked by filling factor $\nu = 8, 10, 12, 14, 16$. The inset shows the zoomed-in part of the data shown in (a) near the cyclotron resonance. A series of deep (shallow) radiation-induced minima is marked by vertical lines (arrows).

FIG. 2. $\rho(B)$ at different f, as marked, measured in sample A. Some examples of MPRs are marked by arrows. The traces are offset for clarity by 7 Ω.

In Fig. 1(a)[(b)], we show magnetoresistance $\rho(B)$ under microwave irradiation of frequency $f = 378$ GHz measured in sample A [B] at $f = 378$ [333] GHz and $T \approx 0.38$ [0.31] K. In both samples, the data reveal microwave-induced resistance oscillations (MIROs) [2,23–25] and SdHOs coexisting over a wide magnetic field range [26]. In addition to MIROs and SdHOs, both data sets show a structure consisting of multiple sharp features in the vicinity of the cyclotron resonance.

A closer look at this structure, shown in the inset of Fig. 1(a), reveals that it is a series of extrema. Near the SdHO maxima, this series is represented by resistance minima which are roughly equally spaced in the magnetic field; between filling factors $\nu = 12$ and $\nu = 14$, we observe at least seven such minima. The minima can be divided into two classes, i.e., strong ones (cf. vertical lines) and weak ones (cf. ↓), appearing roughly in the middle between the neighboring strong minima. As discussed below, these strong (weak) features originate from magnetoplasmon resonances of odd- (even)-order n, with n as high as 25. While the feature around $\nu = 10$ in Fig. 1(a) also originates from photoresistance, identifying its exact nature is left for future studies. One possible origin is the plasmon-photon mode hybridization, which leads to crossing of magnetoplasmon dispersion with cyclotron lines [18,27].
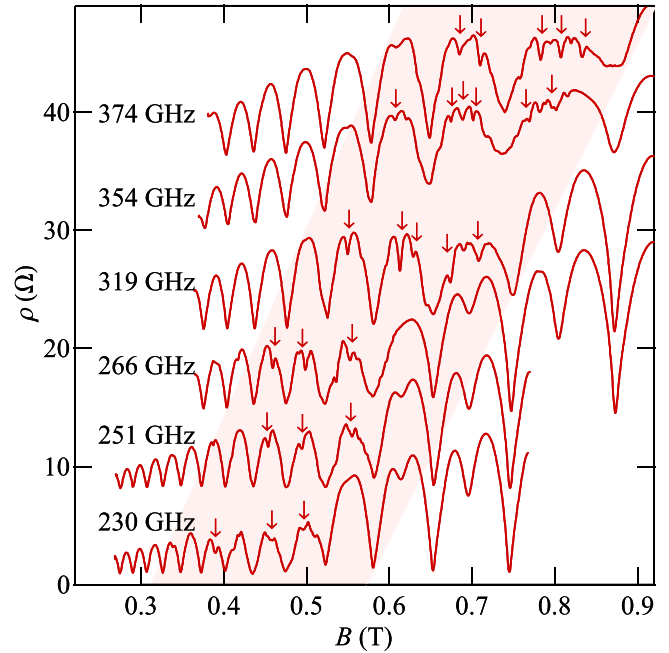
Around the SdHO minima, MPRs are manifested by local maxima [see, e.g., a maximum at $B \approx 7.5$ kG in the inset of Fig. 1(a)]. These maxima are less pronounced due to a weaker temperature dependence of the SdHO resistance minima in the regime of separated Landau levels. Indeed, at even ν, the density of electron states is small in a wide band around the Fermi level and raising the temperature has little effect as long as it remains small compared to interlevel spacing.

In Fig. 2, we plot magnetoresistance $\rho(B)$ measured in sample A at several frequencies from 230 to 374 GHz, as marked [28]. Each trace reveals a series of extrema (some examples marked by an arrow), similar to that shown in Fig. 1, which move to higher B with increasing f. Since the resonances are most pronounced around the SdHO maxima, these extrema are best observed at higher f (lower ν) where more MPR modes can be resolved within one SdHO period. One remarkable feature of our data is the unusually large number of both odd and even MPR modes, made possible by high sensitivity of SdHOs to variations of electron temperature due to resonant absorption in our high-mobility samples [29].

To confirm that the observed extrema originate from MPRs, we examine the dispersion relation for two radiation frequencies using the data from sample A. Per Eq. (1), the magnetic field at which the nth MPR ($\omega = \omega_n$, $B = B_n$) occurs should satisfy

$$B^2 = B_n^2 \equiv (m^\star/e)^2 \left[\omega^2 - n\Omega_1^2 \right]. \tag{4}$$

In Fig. 3, we plot the square of the magnetic field, at which the nth MPR occurs, for $f = 377$ and $f = 354$ GHz, as marked, as a function of n. Here, filled (open) circles represent odd (even) n, spanning from $n = 5$ to $n = 27$ [30]. Despite slight deviation at low n, the data for both frequencies conform to Eq. (4); linear fits generate $m^\star \approx 0.066 m_0$ [31] and $F_1 \approx$
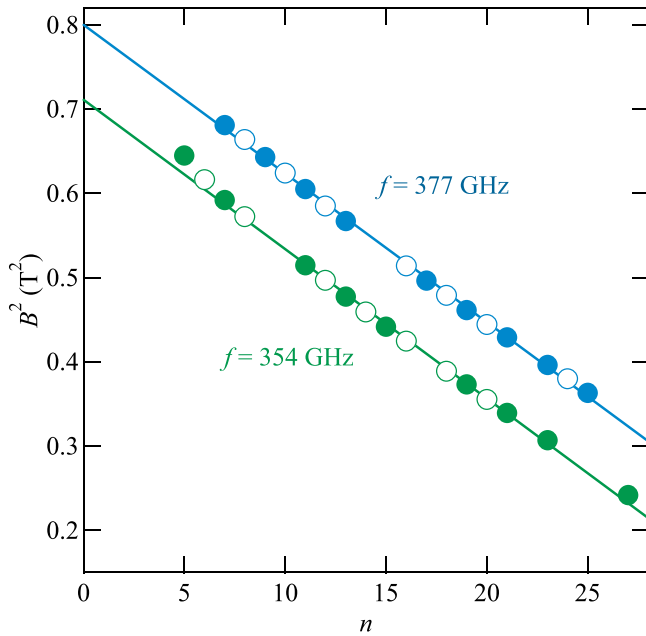
FIG. 3. B^2 (circles) vs n, for $f = 377$ GHz (upper) and 354 GHz (lower), obtained from sample A. Solid (open) circles represent odd (even) n. Fits to the data (lines) using Eq. (4) yield $m^\star \approx 0.066m_0$ and $F_1 \approx 56$ GHz.
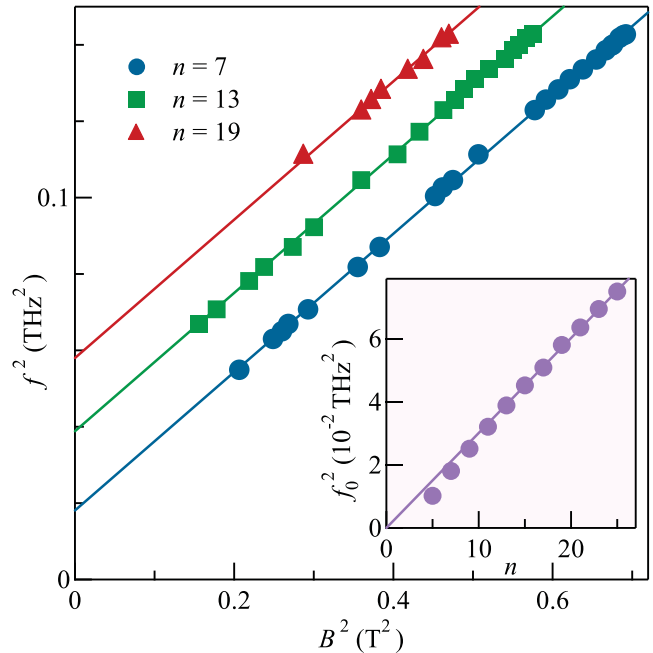

FIG. 4. f^2 vs B^2 for $n = 7$ (circles), 13 (squares), and 19 (triangles), obtained from sample A. The fits to the data (lines) with $f^2 = f_0^2 + (e/2\pi m^\star)^2 B^2$ yield $m^\star = 0.066m_0$. The inset shows f_0^2, obtained from the fits vs n, revealing linear relationship $f_0^2 \sim n$. The slope of the linear fit (line) yields $F_1 \approx 55$ GHz.

56 GHz. Obtained F_1 is about 0.95 of what is expected from Eq. (1), in reasonable agreement with past theoretical [32] and experimental [1,4,9] studies.

We next examine the frequency dependence of the observed resonances and demonstrate that it can also be well described by the magnetoplasmon dispersion, given by Eq. (1). In Fig. 4, we plot f^2 vs B^2 for three select modes, $n = 7,13,19$, and observe that the data can be well described by parallel lines. Such a behavior is indeed expected for MPRs since

$$\omega^2 = \omega_n^2 \equiv n\Omega_1^2 + (e/m^\star)^2 B^2; \qquad (5)$$

see Eq. (1). The universal slope of the linear fits again conforms to $m^\star \approx 0.066m_0$.

After performing such fits for all available n, we extract the intercepts of the fits with the vertical axis f_0^2 and present the result as a function of n in the inset of Fig. 4. The data reveal a linear relation between f_0^2 and n, in accordance with Eq. (1), and from the slope of the fit, $f_0^2 = nF_1^2$, we find $F_1 \approx 56$ GHz, in good agreement with the value obtained above. We further note that at $n < 10$, $f_0^2(n)$ slightly deviates from the linear dependence and bends down. As we show below, this deviation is likely due to retardation effects.

The retardation effects are characterized by the retardation parameter α', defined as the ratio of the plasmon frequency to the light frequency at the same wave number. At the fundamental plasmon wave number $q_1 = \pi/w$, we find, for sample A, $\omega_{ph}/2\pi = c/2wn^\star \approx 0.33$ THz and $\alpha' = \Omega_1/\omega_{ph} \approx 0.07(E_F/\hbar\omega_{ph})^{1/2} \approx 0.18$. Since the phase velocity of the magnetoplasmon mode is proportional to $n^{-1/2}$, the retardation effects become weaker at higher n. It has been shown that the plasmon frequency decreases with α' [4,27]. It is therefore reasonable to have a larger deviation from Eq. (1) at lower n, as observed in both Fig. 3 and Fig. 4(b).

As mentioned in the introduction, observation of multiple MPR modes relies on their sharpness. We estimate the half width of the observed MPR as $\delta B_n \approx 2.5$ mT, which is largely insensitive to n. Since the width is obtained from magnetoresistance, it does not directly translate to the width of the MPR. Nevertheless, since the width of the photoresistance minima does not show significant variation within one SdHO period, it should be comparable to the actual MPR width. Using $\delta\omega_n \approx (\partial\omega_n/\partial B)\delta B_n = (e/m^\star)(\omega_c/\omega)\delta B_n$, we estimate $\delta\omega_n/2\pi \simeq 1$ GHz, close to the cyclotron resonance.

The MPR width $\delta\omega_n$ is expected to be a sum of coherent radiative decay rate Γ_n and incoherent collisional rate γ; see Eq. (2) and Eq. (3). In sample A, we estimate $\Gamma_0/2\pi \approx 14$ GHz and, at $f = 0.38$ GHz, $\Gamma_1/2\pi = \Gamma_0/2\pi(w/\lambda)^2 \approx 4.7$ GHz. At higher n, $\Gamma_n = \Gamma_1/n^2$ becomes smaller than γ. This is consistent with our observation that the fundamental MPR $n = 1$ is not well resolved, whereas higher-order MPRs have similar widths, dominated by γ.

The incoherent scattering rate γ is often associated with the transport scattering rate τ^{-1}, which is about $\tau^{-1}/2\pi \approx 0.2$ GHz in sample A. However, there exists no exact relation between the two quantities; for the electron density of sample A, Ref. [33] has found γ to be about five times larger than τ^{-1}, giving a conservative estimate of $\gamma/2\pi \simeq 1$ GHz. This value is in good agreement with $\delta\omega_n/2\pi \simeq 1$ GHz obtained from our experimental data.

Another interesting feature revealed by our data is the even-odd mode alternating strength [34]. Assuming a uniform electric field distribution, only odd modes are expected [32], consistent with some experiments [1,4]. Other experiments, however, revealed both odd and even low-order modes, with
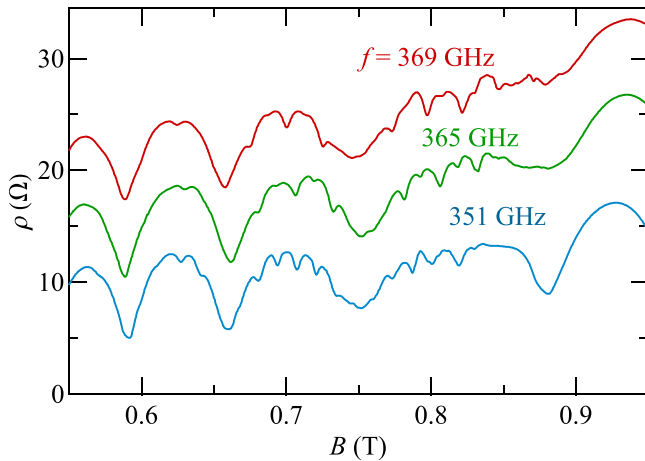
FIG. 5. $\rho(B)$ at $T \approx 0.4$ K and different f, as marked, measured in sample A. Traces are offset for clarity by 7 Ω.

comparable, but often random, strengths [6,14,15]. While we have clearly observed different signal strengths for even and odd modes, their ratio can vary with the radiation frequency. In Fig. 5, we present $\rho(B)$ measured in sample A at different f: 369, 365, and 351 GHz. At $f = 369$ GHz (top trace), the even modes are much weaker than the odd modes; at $f = 365$ GHz (middle trace), they become noticeably stronger; and at $f = 351$ GHz (bottom trace), the even modes become comparable to the odd ones. The variation in the strength of even modes with f likely reflects variation in radiation distribution [35].

While a more uniform radiation produces weaker even modes, they become more pronounced under nonuniform radiation distribution. Our measurements never revealed even modes that are stronger than the odd ones.

In summary, exploiting high-mobility 2DEGs, high radiation frequencies, and strong sensitivity to temperature of SdHOs, we have detected high-order magnetoplasmon resonances. Extending to orders above $n = 25$, the MPR-induced photoresistance extrema exhibit alternating strength, being less (more) pronounced at even (odd) n. Taken together, our results demonstrate that this experimental technique provides a surprisingly sensitive and elegant means to detect and investigate high-order MPR modes which could be applicable to other 2D systems, such as MgZnO/ZnO heterojunctions [36] and AlAs quantum wells [37].

[1] E. Vasiliadou, G. Müller, D. Heitmann, D. Weiss, K. von Klitzing, H. Nickel, W. Schlapp, and R. Lösch, Phys. Rev. B **48**, 17145 (1993).

[2] M. A. Zudov, R. R. Du, J. A. Simmons, and J. L. Reno, Phys. Rev. B **64**, 201311(R) (2001).

[3] S. Holland, C. Heyn, D. Heitmann, E. Batke, R. Hey, K. J. Friedland, and C.-M. Hu, Phys. Rev. Lett. **93**, 186804 (2004).

[4] I. V. Kukushkin, V. M. Muravev, J. H. Smet, M. Hauser, W. Dietsche, and K. von Klitzing, Phys. Rev. B **73**, 113310 (2006).

[5] C. L. Yang, R. R. Du, L. N. Pfeiffer, and K. W. West, Phys. Rev. B **74**, 045315 (2006).

[6] S. I. Dorozhkin, A. A. Bykov, I. V. Pechenezhskii, and A. K. Bakarov, JETP Lett. **85**, 576 (2007).

[7] L.-C. Tung, C. L. Yang, D. Smirnov, L. N. Pfeiffer, K. W. West, R. R. Du, and Y.-J. Wang, Solid State Commun. **149**, 1531 (2009).

[8] I. V. Andreev, V. M. Muravev, I. V. Kukushkin, S. Schmult, and W. Dietsche, Phys. Rev. B **83**, 121308(R) (2011).

[9] A. T. Hatke, M. A. Zudov, J. D. Watson, and M. J. Manfra, Phys. Rev. B **85**, 121306(R) (2012).

[10] A. T. Hatke, M. A. Zudov, J. D. Watson, M. J. Manfra, L. N. Pfeiffer, and K. W. West, Phys. Rev. B **87**, 161307(R) (2013).

[11] MPRs can also be observed directly in microwave absorption [4,14].

[12] F. Stern, Phys. Rev. Lett. **18**, 546 (1967).

[13] A. V. Chaplik, Sov. Phys. JETP **35**, 395 (1972).

[14] S. A. Studenikin, A. S. Sachrajda, J. A. Gupta, Z. R. Wasilewski, O. M. Fedorych, M. Byszewski, D. K. Maude, M. Potemski, M. Hilke, K. W. West et al., Phys. Rev. B **76**, 165321 (2007).

[15] I. Baskin, B. M. Ashkinadze, E. Cohen, and L. N. Pfeiffer, Phys. Rev. B **84**, 041305 (2011).

[16] M. Bialek, M. Czapkiewicz, J. Wrobel, V. Umansky, and J. Lusakowski, Appl. Phys. Lett. **104**, 263514 (2014).

[17] The photovoltage measured in Ref. [16] revealed maxima at the positions corresponding to a subset of modes. For example, at $f = 645$ GHz, this subset includes modes 3,7,9,11,15, but not 1,5,13,17,19. A similar conclusion holds for other data shown in Fig. 2 of Ref. [16].

[18] V. M. Muravev, I. V. Andreev, S. I. Gubarev, V. N. Belyanin, and I. V. Kukushkin, Phys. Rev. B **93**, 041110(R) (2016).

[19] K. W. Chiu, T. K. Lee, and J. J. Quinn, Surf. Sci. **58**, 182 (1976).

[20] S. A. Mikhailov, Phys. Rev. B **54**, 10335 (1996).

[21] Q. Zhang, T. Arikawa, E. Kato, J. L. Reno, W. Pan, J. D. Watson, M. J. Manfra, M. A. Zudov, M. Tokman, M. Erukhimova et al., Phys. Rev. Lett. **113**, 047601 (2014).

[22] R. P. Leavitt and J. W. Little, Phys. Rev. B **34**, 2450 (1986).

[23] R. G. Mani, J. H. Smet, K. von Klitzing, V. Narayanamurti, W. B. Johnson, and V. Umansky, Nature (London) **420**, 646 (2002).

[24] M. A. Zudov, R. R. Du, L. N. Pfeiffer, and K. W. West, Phys. Rev. Lett. **90**, 046807 (2003).

[25] C. L. Yang, M. A. Zudov, T. A. Knuuttila, R. R. Du, L. N. Pfeiffer, and K. W. West, Phys. Rev. Lett. **91**, 096803 (2003).

[26] Q. Shi, P. D. Martin, A. T. Hatke, M. A. Zudov, J. D. Watson, G. C. Gardner, M. J. Manfra, L. N. Pfeiffer, and K. W. West, Phys. Rev. B **92**, 081405(R) (2015).

[27] I. V. Kukushkin, J. H. Smet, S. A. Mikhailov, D. V. Kulakovskii, K. von Klitzing, and W. Wegscheider, Phys. Rev. Lett. **90**, 156801 (2003).

[28] While at different f we sometimes detect variations of electron density of ∼1% due to different power, these variations have a negligible effect on the MPR dispersion.

[29] In addition to heating, another possible contribution to the signal is the MPR-induced spatial density variations [15]. As such variations occur on the length scale set by the magnetoplasmon wavelength, it would also suppress SdHOs which are measured over larger length scales.

[30] Lower-order MPRs overlap with the cyclotron resonance absorption peak [18] which causes strong SdHO suppression, making them insensitive to minute temperature changes caused by MPRs. Gaps in the data correspond to B_n away from the SdHO maxima, where the resonances were not well resolved.

[31] Consistent with previous studies [10], this value is about 10% larger than the one obtained from MIROs.

[32] S. A. Mikhailov and N. A. Savostianova, Phys. Rev. B **71**, 035320 (2005).

[33] I. V. Andreev, V. M. Muravev, V. N. Belyanin, and I. V. Kukushkin, Appl. Phys. Lett. **105**, 202106 (2014).

[34] Interestingly, the strength of MPR-induced photoresistance dips shows little variation with odd or even n.

[35] Our experiments are performed without using resonant cavities and, as a result, the radiation field distribution is not controllable. Furthermore, the presence of contacts, metallic pins on the chip carrier, and other metallic parts make random formation of standing waves in the sample space possible. At 0.4 THz, the distance between the nodes of such standing waves is close to or smaller than the sample dimensions. As a result, different parts of the sample are exposed to different radiation intensities.

[36] V. E. Kozlov, A. B. Van'kov, S. I. Gubarev, I. V. Kukushkin, V. V. Solovyev, J. Falson, D. Maryenko, Y. Kozuka, A. Tsukazaki, M. Kawasaki *et al.*, Phys. Rev. B **91**, 085304(R) (2015).

[37] V. M. Muravev, A. R. Khisameeva, V. N. Belyanin, I. V. Kukushkin, L. Tiemann, C. Reichl, W. Dietsche, and W. Wegscheider, Phys. Rev. B **92**, 041303(R) (2015).